RSC Advances

ROYAL SOCIETY OF CHEMISTRY

www.rsc.org/advances

Journal Name

ARTICLE

Alkyl bisimidazolium-mediated crosslinked comb-shaped polymers as highly conductive and stable anion exchange membranes

Anil H. N. Rao,[a] SangYong Nam[b] and Tae-Hyun Kim[*,a]

Crosslinked poly(arylene ether sulfone)s (PES) with pendant alkyl bisimidazolium units, which acted as both crosslinkage sites and hydroxide conductors, were developed as anion exchange membranes (AEMs). These bisimidazolium-mediated crosslinked membranes (BI-cPESs) displayed a high hydroxide conductivity exceeding 0.012 S/cm at 20°C and 0.061 S/cm at 80°C, together with good chemical, thermal, mechanical, oxidative and dimensional stabilities. The BI-cPES membrane, which included a long alkyl chain (C_{10}, BI-cPES-10), formed self-aggregated structures due to the long pendant hydrophobic side chain that formed a comb shape. The benefit of this crosslinked comb-shaped system was its high conductivity of 0.027 S/cm at 20°C, even at an IEC as low as 1.13 meq/g and a low water uptake of 8.70%.

Introduction

Anion exchange membrane-based alkaline fuel cells (AEMFCs) have attracted increasing attention due to their advantages over the more well-known and well-developed proton exchange membrane-based fuel cells (PEMFCs). The advantages of AEMFCs include the avoidance of precious metal-based electrode catalysts, fast oxygen reduction kinetics at the cathode, reduced corrosion, and the use of inexpensive metal hardware due to the high pH of the operating conditions [1-4].

A variety of polymers, including poly(ether sulfone)s [5,6], poly(ether ketone)s [7,8], polyimides [9], poly(phenylene oxide)s [10-12], and hybrid composites involving inorganic materials [13], have been utilized as base polymers for AEMs. Quaternized ammonium [14-16], guanidinium [17], piperazinium [18], morpholinium [19], and imidazolium salts [20-23] have been tethered onto these polymers in an effort to introduce hydroxide conducting groups. Despite the ease with which these polymers may be prepared and their properties tuned, these systems are limited with respect to their practical utility in AEMFCs by their poor stabilities under alkaline (high pH) conditions. AEM development is also challenged by difficulties associated with achieving a high OH^- ion conductivity due to the low electrochemical mobility of OH^- ions in water, relative to the mobility of H^+. The simplest and most direct approach to maximizing OH^- ion conductivity in AEMs involves increasing the ion exchange capacity (IEC), defined as the milliequivalents (meq) of conducting groups per gram of polymer. A high IEC is inevitably accompanied by a significant increase in the water uptake, which can lead to uncontrolled dimensional swelling, loss of mechanical properties, or even disintegration of AEM, especially at high temperatures.

We recently introduced a class of poly(arylene ether sulfone)s, in which long pendant hydrophobic side chains were introduced onto the imidazolium cation to produce comb-shaped, hydroxide-conducting polymers [24]. AEMs based on this comb-shaped system caused ion aggregation and successfully controlled both the IEC and morphology of the polymer membranes. The formation of a large ionic cluster resulted in a very high hydroxide conductivity through the alkyl imidazolium-functionalized comb-shaped membranes.

Crosslinking is an effective method of stabilizing PEMs [25-27] or AEMs [28,29], especially those with a high IEC, against water swelling. In the absence of crosslinking, these polymers would swell significantly, causing unacceptable water uptake and large dimensional variations and resulting in inadequate mechanical properties. Crosslinking, however, frequently reduces ionic conductivity, and few crosslinked membranes provide both a high conductivity and good dimensional/mechanical stability [30-35].

The present work aimed to combine the advantages of crosslinking and the ion-aggregation characteristics of comb-shaped polymers by developing a novel poly(arylene ether sulfone) with pendant alkyl bisimidazolium groups on the polymer side chains as crosslinkers, **1**. Crosslinkages provided a three-dimensional structure of crosslinked polymer membranes in which the pendant bisimidazolium groups acted as both crosslinking units and ion conductors. The resulting crosslinked comb-shaped membranes showed excellent physicochemical stabilities, together with a high conductivity, even at a low IEC.

The bisimidazolium-mediated crosslinked PES membranes (BI-cPESs, **1**) were simply and efficiently prepared through a nucleophilic substitution reaction between the precursor polymer (bromobenzylated PES, Br-PES) with alkyl bisimidazoles bearing three different alkyl chains. Although a few membranes based on the comb-shaped polymers have been reported [24, 36-39], this is the first example of crosslinked comb-shaped polymers based on the alkyl bisimidazolium cation. The effects of the alkyl chains in the bisimidazolium groups on the morphologies and properties of the polymers, as well as on the properties of the corresponding anion exchange membranes, were thoroughly investigated.

Structure 1 here

Experimental

Materials

Bis-(4-fluorophenyl)-sulfone (FPS) was obtained from Aldrich Chemical Co. 2,2-Bis(4-hydroxyphenyl)-hexafluoropropane (6-FBPA) was purchased from TCI and used as obtained. Potassium carbonate, FPS, 6-FBPA were dried under vacuum at 60 °C for 24 h prior to the polymerization. Phenolphthalein (PP), 1,4-dibromobutane, 1,6-dibromohexane, 1,10-dibromodecane and 3,5-dimethylaniline (DMA) were obtained from Aldrich Chemical and used as obtained. The bisimidazole derivatives were synthesized according to the reported procedure by reacting imidazole with corresponding dibromo alkanes in presence of NaH [40]. 2-(3,5-Dimethylphenyl)-3,3-bis(4-hydroxyphenyl)isoindolin-1-one was synthesized according to the literature procedure [41] by reacting DMA with PP in its acid form. All other chemicals were obtained from commercial sources and used without further purification. Distilled water was used throughout this study.

Characterization

^{1}H NMR spectra were obtained on an Agilent 400-MR (400 MHz) instrument using d_6-DMSO or CDCl$_3$ as a reference or internal deuterium lock. FT-IR spectra were recorded on a Nicolet MAGNA 560-FTIR spectrometer. Molar masses were determined either by comparative spectroscopic methods using ^{1}H NMR or Gel Permeation Chromatography (GPC) using two PL Gel 30 cm × 5 μm mixed C columns at 30 °C running in DMF and calibrated against polystyrene (M_n = 600-10^6 g/mol) standards using a Knauer refractive index detector. The X-ray diffraction patterns of the dry membranes were recorded using a Rigaku HR-XRD smartlab diffractometer by employing a scanning rate of 0.1°/min in a 2θ range from 0° to 1.5° with a Cu-Kα X-ray (λ = 1.54 Å). The dried membranes were placed under vacuum at 80 °C for 24 h prior to the measurement. Tapping mode Atomic Force Microscopy (AFM) was performed using a Bruker MultiMode instrument. A silicone cantilever with an end radius <10 nm and a force constant of 40 N/m (NCHR, nanosensors, f=300 kHz) was used to image the samples at ambient temperature. The samples were equilibrated with 50% RH at least 24 h prior to the imaging. The measurements were conducted under the same conditions for each sample to keep consistency. Thermal stability of the hydroxide form membranes was analyzed by the thermogravimetric analysis measurements on a Shimadzu TGA-2950 instrument at a heating rate of 10 °C min^{-1} in a nitrogen flow. Tensile properties were measured on a Shimadzu EZ-TEST E2-L instrument benchtop tensile tester using a crosshead speed of 1 mm/min at 25 °C under 50% relative humidity. The membranes have a thickness between 40 and 50 μm. Engineering stress was calculated from the initial cross sectional area of the sample and Young's modulus (E) was determined from the initial slope of the stress-strain curve. The membrane samples were cut into a rectangular shape with 80 mm × 8 mm (total) and 80 mm × 3 mm (test area)

Synthesis of the bromobenzylated poly(arylene ether sulfone) precursor polymer (Br-PES)

Synthesis of the OH-terminated oligomer 3 with D.P. of 12

2-(3,5-Dimethylphenyl)-3,3-bis(4-hydroxyphenyl)isoindolin-1-one (7.2 g, 17.09 mmol), FPS (4.0 g, 15.73 mmol) and potassium carbonate (4.74 g, 34.35 mmol) were added to a mixture of DMAc (25 cm^3) and toluene (30 cm^3) in a 250 cm^3 round bottom flask equipped with a Dean-Stark apparatus and a nitrogen inlet. The reaction mixture was heated at 150 °C for 4 h. After azeotropic distillation, toluene was collected before the temperature was raised to 170 °C and stirred for 16 h under nitrogen. At the end of the reaction, a small amount of 2-(3,5-dimethylphenyl)-3,3-bis(4-hydroxyphenyl)isoindolin-1-one was added to ensure the end capping. The reaction mixture was, then, cooled to r.t. and dissolved in DMF (15 cm^3), followed by pouring into a 1:1 mixture of ethanol and HCl (500 cm^3). The product was collected by filtration and washed with deionized water several times before drying at 80 °C under vacuum for at least 48 h to give the hydroxy-terminated oligomer **3** as a white powder (9.4 g, 83.0%); δ_H (400 MHz, CDCl$_3$) 8.00 (3H, d, J=8.0Hz, ArH_6), 7.86 (12H, d, J=8.0Hz, ArH_{2b}) 7.59-7.50 (7H, m, ArH_5), 7.36 (1H, d, J=8.0Hz, ArH_a), 7.23-7.20 (16H, m, ArH_1), 6.98 (14H, d, J=8.0Hz, ArH_3), 6.91 (12H, d, J=8.0Hz, ArH_4), 6.84 (4H, s, ArH_8), 6.46 (6H, s, ArH_9) and 2.14 (20H, s, CH$_3H_7$); (KBr)/cm^{-1} 3430, 2920, 1685, 1668, 1590, 1485, 1295, 1150 and 835.

Synthesis of the F-terminated oligomer 4 with D.P. of 12

6-FBPA (5.0 g, 14.87 mmol), FPS (3.96 g, 15.60 mmol) and potassium carbonate (4.33 g, 31.35 mmol) were added to a mixture of DMAc (25 cm^3) and toluene (30 cm^3) in a 250 cm^3 round bottom flask equipped with a Dean-Stark apparatus and a nitrogen inlet. The reaction mixture was heated at 150 °C for 4 h, and toluene was distilled out after azeotropic distillation. The temperature was then raised to 170 °C and allowed to stir at this temperature for another 16 h under a nitrogen atmosphere. At the end of the reaction time, a small amount of FPS was added to ensure the end capping. The mixture was cooled to r.t. and dissolved in DMF (10 cm^3), followed by pouring into methanol (500 cm^3). The product was collected by filtration and the residual inorganic materials were removed by treating with deionized water several times. This was repeated twice, and the solid was dried at 80 °C under vacuum for at least 48 h to give the F-terminated oligomer **4** as a white solid (7.8 g, 86.6%); δ_H (400 MHz, CDCl$_3$) 7.92 (12H, d, J=8.0Hz, ArH_{13d}) 7.41 (12H, d, J=8.0Hz, ArH_{11}), 7.21-7.16 (1H, m, ArH_c), 7.10 (11H, d, J=8.0Hz, ArH_{10}) and 7.03 (12H, d, J=8.0Hz, ArH_{12}); (KBr)/cm^{-1} 3025, 1588, 1510, 1485, 1275, 1245, 1140, 1110, 870 and 830.

Synthesis of the poly(arylene ether sulfone) (PES) multiblock copolymer 5

The OH-terminated oligomer (**3**) (4.0 g, 0.49 mmol) and the F-terminated oligomer (**4**) (3.40 g, 0.49 mmol) were mixed with potassium carbonate (0.15 g, 1.04 mmol) in a 250 cm^3 round bottom flask equipped with a Dean-Stark apparatus and a nitrogen inlet. DMAc (35 cm^3) and toluene (30 cm^3) were added and the reaction mixture was heated at 150 °C to essentially remove water by azeotropic distillation. After 4 h, toluene was distilled out, and the temperature of the reaction mixture was raised to 170 °C. This was left to stir at this temperature for another 18 h under a nitrogen atmosphere. After this time, the mixture was cooled to r.t. and dissolved in DMF (20 cm^3). The reaction mixture was poured into methanol (700 cm^3). The product was collected by filtration and washed several times with deionized water to remove the residual inorganic materials. The solid was dried at 80 °C under vacuum for at least 48 h to give the multiblock copolymer (**5**) as white

beads (6.8 g, 91.8%); δ_H (400 MHz, CDCl$_3$) 8.01-7.99 (1H, br signal, ArH_{19}), 7.93-7.85 (8H, br signal, Ar$H_{15,15'}$), 7.59-7.50 (2H, m, ArH_{18}), 7.41-7.39 (4H, br signal, ArH_{24}), 7.23-7.19 (5H, br signal, ArH_{14}), 7.11-7.09 (4H, br signal, ArH_{23}), 7.04-6.97 (8H, br signal, Ar$H_{16,17}$), 6.92-6.90 (4H, br signal, ArH_{25}), 6.84 (1H, br signal, ArH_{21}), 6.47 (2H, br signal, ArH_{22}) and 2.14 (6H, s, 2×CH_3H_{20}); (KBr)/cm^{-1} 3067, 3034, 2962, 1670,1590, 1488, 1325, 1241, 1169, 1148, 873 and 834; GPC (DMF, RI)/Da M_n 1.38×10^5, M_w 2.40×10^5 and M_w/M_n 1.74.

Bromination of the PES copolymer to give the Br-PES 2

In a 500 cm^3 two-necked flask equipped with a magnetic stirrer, a nitrogen inlet and a condenser, the multiblock copolymer (**5**) (6.5 g, 0.43 mmol) was dissolved in 1,1,2,2-tetrachloroethane and gently heated to dissolve completely. A catalytic amount of benzoyl peroxide (BPO) and N-bromosuccinimide (NBS) (3.03 g, 17.06 mmol) were then added in small amounts to avoid side reactions. The reaction mixture was further heated to 85 ℃ for 8 h. After cooling to r.t., the solution was precipitated into methanol (750 cm^3) and the solid was collected by filtration, washed with water and dried at 80 ℃ under vacuum for at least 24 h to give the brominated PES copolymer (**2**) as a yellow solid (6.0 g, 82%); δ_H (400 MHz, CDCl$_3$) 8.03-8.01 (1.72H, br signal, ArH_{19}), 7.93-7.84 (12.8H, br signal, Ar$H_{15,15',18}$), 7.62-7.54 (3.6H, m, ArH_{23}), 7.41-7.23 (16H, br signal, Ar$H_{16,17}$), 7.11-6.96 (25H, br signal, Ar$H_{24,25,21,22}$), 4.45 (3.2H, br signal, 0.83×2×ArCH_2Br,H_{26}) and 2.29 (1H, s, 0.17×2×Ar$CH_3H_{20'}$); (KBr)/cm^{-1} 3074, 2970, 1672,1590, 1480, 1315, 1235, 1150, 875, 830 and 653.

Fabrication of the bisimidazolium-mediated crosslinked PES (BI-cPES) membranes

The simultaneous quaternization and crosslinked AEMs were prepared as follows. To a solution of Br-PES polymer **5** (0.4 g) in 8.0 cm^3 of dry DMF was added bisimidazole derivatives (0.41 mmol) and stirred at r.t. for 15 min to obtain a homogeneous solution. The solution was then filtered through a cotton plug before pouring onto a glass plate and drying under oven at 80 ℃ for 12 h, then membrane was vacuum dried at 80 ℃ for 8h to evaporate the residue solvent. The membrane thickness was well controlled by means of a doctor blade. The membranes were peeled off by immersion in deionized water, and the resultant membrane was immersed in 1 M NaOH in a closed container for 48 h at r.t. to exchange with OH$^-$. Finally, the obtained membrane was immersed in deionized water for 48 h prior to any measurements.

Measurements

Ion exchange capacity (IEC). The IEC of the AEMs was determined by the back titration method. 0.03 g of the membrane samples were equilibrated with 35 cm^3 of 0.01 M HCl standard solution for 48 h, followed by back titration of 0.01 M NaOH standard solution with phenolphthalein as an indicator. The measured IEC value was calculated using the following equation:

$$IEC \ (meq/g) = (V_{0NaOH}C_{NaOH} - V_{XNaOH}C_{NaOH})/W_{dry}$$

, where V_{0NaOH} and V_{xNaOH} are the volume of the NaOH consumed in the titration without and with membranes respectively, C_{NaOH} is the mole concentration of the NaOH which are titrated by the standard oxalic acid solution, and W_{dry} is the weight of the dried membranes. Three trials were conducted for each sample. The IEC, water uptake and swelling ratios were obtained by the average of 3 different measurements. The theoretical IEC was calculated from the total molecular weight of one block copolymer repeating unit multiplied with degree of functionalization.

Water uptake (WU, %). The WU of the AEMs was measured as follows: after soaking the membranes in distilled water for more than 24 h, they were wiped with a filter paper and weighed immediately (W_{wet}). The membranes were then dried under a vacuum condition until a constant weight was obtained (W_{dry}). The water uptake of the membranes was calculated by following equation:

$$WU \ (\%) = [(W_{wet} - W_{dry})/W_{dry}] \times 100$$

, where, W_{wet} and W_{dry} are the weight of wet membrane and weight of dry membrane respectively.

Dimensional change of the membranes was evaluated from measuring the swelling ratio of the membranes, which was investigated by immersing the round-shaped membranes into water at r.t. and 80 °C, respectively, and the changes of through-plane direction were calculated using the following equations:

$$\Delta t \ (\%) = [(t - t_{dry})/t_{dry}] \times 100$$

, where t_{dry} is the thickness of the dried membranes, and t refers to that of the membranes immersed in water for 24 h. The dried membranes were prepared by placing membranes under vacuum at 60 °C for 24 h prior to the measurement.

Conductivity. Hydroxide ion conductivity (σ) in plane direction of each membrane (size: 1cm × 4cm in liquid water) was obtained using σ = l/RA (l: distance between reference electrodes, A: cross-sectional area of a membrane coupon). Here, ohmic resistance (R) was measured by two-point probe alternating current (ac) impedance spectroscopy using an electrode systems connected with an impedance/gain-phase analyzer (SI-1260) and an electrochemical interface (SI-1287) over the frequency range from 10 to 200 kHz. The conductivity measurements in liquid water were performed at different temperature range from 20 ℃ to 80 ℃. To minimize unwanted carbonate formation, the cell was completely immersed in degassed and deionized water and the impedance spectrum was collected quickly. The conductivity value was obtained by the average of at least 3 trials with same time intervals.

Chemical stability. Chemical stability of the membranes was evaluated by immersing the OH$^-$ form membranes into stirred 2 M NaOH solution at 60 °C for up to 350 h to measure the changes in ionic conductivity, IEC and IR spectra. Before measurements, each membrane was washed with deionized water several times and soaked in deionized water for at least 48 h at r.t. to remove the free NaOH inside the membrane. The ionic conductivity of each membrane was determined in deionized water at 20 °C.

Oxidative stability. Oxidative stability of the membranes was evaluated in Fenton's reagent (3 wt% H$_2$O$_2$ containing 3 ppm FeSO$_4$). The membranes were soaked in Fenton's reagent at 60 °C for 250 h. After every 50 h, membranes were dried with filter paper to remove the surface liquid and the weight of each membrane was recorded.

Results and Discussion

Synthesis and characterization of the PES multiblock copolymer (PES) and its brominated form (Br-PES)

The synthetic route to the bromobenzylated multiblock poly(arylene ether sulfone) (Br-PESs, **2**) is illustrated in Scheme 1.

Scheme 1 here

We previously introduced a cardo-based biphenol monomer with a dibenzyl functionality **S1** (see Scheme S1 in ESI[†]) prepared through the reaction of phenolphthalein (PP) with 3,5-dimethyl aniline (DMA) (Scheme S1 and Figure S1 in ESI[†]) [23]. This cardo monomer separates the reactive benzylic sites, at which the ionic conductor is to be introduced, from the polymer backbone, and offers two such reactive sites for further functionalization that is, an bisimidazolium group. The OH- and F-terminated telechelic oligomers (**3** and **4**) were prepared according to the literature procedures [23], with the degree of polymerization (D.P.) of each oligomer fixed at 12. Polymerization using these two macromonomers produced the poly(arylene ether sulfone) block copolymer (PES) **5** with a high molecular weight (M_n > 124 kDa, as confirmed by GPC in Figure S2 in ESI[†]), supporting the formation of a multiblock structure.

Figure 1 here

The chemical structure of the multiblock copolymer **5** was characterized by ^{1}H NMR spectroscopy by reference to the spectra of the two starting oligomers **3** and **4** (Figure S3 in ESI[†]). Bromination of the ArCH$_3$ unit using 1.5 equiv. of NBS was conducted in a tetrachloroethane solution of polymer **5** to produce bromobenzylated PES (Br-PES) **2**. Comparative ^{1}H NMR spectroscopic analysis of the polymers **5** and **2** revealed that the degree to which polymer **2** was brominated, estimated from the integral ratio of the bromobenzyl protons (H$_{26}$) in **5** to the benzylic protons (H$_{20}$) in **2**, was 74% (Figure 1).

Preparation and characterization of the bisimidazolium-mediated crosslinked membranes (BI-cPESs)

The bisimidazolium-mediated crosslinked membranes (BI-cPESs, **1**) were prepared by reacting the Br-PES **2** with 2.0 equivalents of three different alkyl bridged bisimidazoles (bisimidazole with butyl, hexyl, and decyl group, designated BI-4, BI-6 and BI-10, respectively) in a DMF solution, followed by membrane casting and thermal drying for 12 h (Scheme 2). During the drying process, the reactive benzyl bromide group in polymer **2** reacted with the bisimidazole group in BI-4, BI-6, and BI-10 to produce the bisimidazolium-mediated crosslinked PES membranes with three different alkyl chain lengths, designated BI-cPES-4, BI-cPES-6, and BI-cPES-10, respectively (Scheme 2). Subsequent immersion of these membranes into a sodium hydroxide solution offered bisimidazolium-mediated crosslinked membranes with hydroxide counter anions as transparent and flexible membranes (Scheme 2). The membrane thickness was found to be 40–50 μm. The bisimidazolium groups were used as both crosslinkers and ion conductors.

Scheme 2 here

The crosslinked membranes were insoluble in common organic solvents, including DMF, NMP, DMAc, and DMSO, supporting the successful formation of the crosslinked network. The gel fraction, an indirect measurement of the crosslinking density, was very high (92%) for all three crosslinked membranes (BI-cPESs) (Table S1 in ESI[†]).

The structures of the crosslinked membranes were further verified by comparing the FT-IR spectra of Br-PES **2** and the crosslinked BI-cPES membrane **1** (Figure S4 in ESI[†]). The peak at 653 cm^{-1}, corresponding to the C-Br stretching vibration of Br-PES **2**, disappeared, and the characteristic peak at 1590 and 758 cm^{-1}, appeared due to the vibrational mode of the imidazolium cations, indicating the successful incorporation of the imidazolium groups [42,43].

Morphology

A morphological analysis of the bisimidazolium-mediated crosslinked membranes (BI-cPESs) was carried out using atomic force microscopy (AFM) and small-angle X-ray scattering (SAXS) studies. Tapping mode AFM images revealed phase separation between the hydrophilic and hydrophobic blocks for all three crosslinked membranes; however, phase separation was most distinct for the BI-cPES-10 membrane with long alkyl chains than for the BI-cPES-4 and BI-cPES-6. Wider hydrophilic channels were observed in the AFM images of BI-cPES-10, whereas BI-cPES-4 and BI-cPES-6 showed narrower channels (Figure 2 and Table 1).

Figure 2 here

Table 1. AFM and SAXS data obtained from the crosslinked BI-cPES membranes.

Membrane	q-value (Å^{-1})	Ionic domain spacing (nm)	Ionic cluster size from AFM (nm)
BI-cPES-4	0.037	17	8
BI-cPES-6	0.024	26	12
BI-cPES-10	0.021	30	23

The SAXS results are presented in Figure 3 by plotting the intensity as a function of the scattering vector, q, and clear ionomeric peaks were observed at 0.02 Å for BI-cPES-6 and BI-cPES-10, with relatively long alkyl chains apparent in the SAXS profile, indicating the formation of nanophase separation with ionic domains. By contrast, a much broader peak at higher q values was observed for BI-cPES-4 with a short alkyl chain, suggesting that phase separation was less clear for this polymer. The interdomain spacings, d values, were relatively large, between 26 and 30 nm, for BI-cPES-6 and BI-cPES-10 (Table 1). The comb-shaped structures of these crosslinked polymers (BI-cPES-6 and BI-cPES-10), although the comb-structure is less clear for BI-cPES-6, appeared to be responsible for their large d values. The d values of AEMs described elsewhere are typically much smaller [44,45] and comparable to the value of 17 nm obtained from BI-cPES-4 (Table 1).

Figure 3 here

Both the AFM and SAXS results suggested that phase separation between the hydrophilic and hydrophobic aggregates to form ionic clusters was facilitated by the long alkyl chains between the bisimidazolium crosslinker. The self-aggregated morphology induced by the comb-shaped BI-cPES structures with long alkyl chains (i.e., BI-cPES-10) strongly influenced the conductivity and dimensional stability (*vide infra*) of the membrane.

The AFM and SAXS results suggested that the ion conducting pathways became more interconnected as the alkyl chain length

between the two imidazole crosslinkers increased. A higher ion conductivity is, therefore, expected of the bisimidazolium-crosslinked PES membranes with longer alkyl chains (BI-cPES-10>BI-cPES-6>BI-cPES-4).

IEC and hydroxide conductivity

The ion exchange capacity (IEC), measured in meq/g, is an important parameter for determining the performances of AEMs and provides information about the density of ion conducting sites in the membrane. The IEC of the bisimidazolium-mediated crosslinked BI-cPES membranes was evaluated by acid–base titration and was found to be 1.13–1.20 meq/g (Table 2). Increasing the alkyl chain length of the bisimidazolium cation reduced the IEC, with the lowest IEC value obtained for BI-cPES-10 (1.13 meq/g). This effect was due to the increased hydrophobicity of the alkyl chain.

Table 2. IEC, conductivity, and E_a of the crosslinked BI-cPES membranes.

Membrane	IEC (meq/g)	Conductivity (S/cm)				^aE_a
		20 °C	40 °C	60 °C	80 °C	
BI-cPES-4	1.20	0.012	0.026	0.040	0.061	23.0
BI-cPES-6	1.18	0.016	0.034	0.054	0.074	21.8
BI-cPES-10	1.13	0.027	0.050	0.070	0.090	17.1

^aE_a: in kJ/mol

The hydroxide conductivities of the bisimidazolium-mediated crosslinked membranes (BI-cPESs) were measured in water at 20–80 °C (Table 2). The BI-cPES-10 membrane had the longest alkyl chain and showed a very high conductivity exceeding 0.02 S/cm at 20 °C with a low IEC of only 1.13 meq/g. The BI-cPES-10 membrane having the longest alkyl chain showed a very high conductivity exceeding 0.02 S/cm at 20 °C with a low IEC of only 1.13 meq/g. This value was much higher than the values measured among typical AEMs and exceeded the conductivity for other crosslinked AEMs based on benzyl quarternary ammonium cations as conducting groups.[46-49] Unlike most crosslinked systems, in which crosslinks are formed through a hydrophobic network that dilutes the conducting groups, our crosslinked polymers were connected by bisimidazolium groups that also acted as ion conductors. Therefore, crosslinking did not reduce the membrane conductivity.

The interconnected nanochannel pathways formed by phase separation between the hydrophilic and hydrophobic aggregates induced by the comb-shaped structure further increased the conductivity in the membrane crosslinked with long alkyl chains (BI-cPES-10), even at a low IEC value. The SAXS and AFM results both showed that BI-cPES-10 formed the largest ionic channels, in good agreement with the highest conductivity displayed by this membrane.

Figure 4 here

The conductivities of the crosslinked BI-cPES membranes also showed Arrhenius-type behavior with a high temperature dependence (Figure 4 and Table 2). All three crosslinked BI-cPES membranes exhibited conductivities exceeding 0.06 S/cm at 80 °C, higher than the values typical of AEMs with similar IEC values. The apparent activation energies (ΔE_a) of hydroxide conduction, estimated from the slopes of the Arrhenius plots, showed that the activation energy of BI-cPES-10 (17.1 kJ/mol) was significantly lower than those of BI-cPES-4 (23.0 kJ/mol) and BI-cPES-6 (21.8 kJ/mol). This result indicated that a percolation threshold of ion

channels through which hydroxide ions could be transported was achieved in the comb-shaped polymer with long alkyl chains (BI-cPES-10) that self-aggregated to form a network of conducting channels. Indeed, the difference in the conductivities of BI-cPES-4 and BI-cPES-6 was less than the difference between BI-cPES-6 and BI-cPES-10 at every temperature measured (Table 2).

Water uptake and dimensional stability

For most AEMs, water uptake by the membrane is closely related to the hydroxide conductivity, as water molecules act as carriers for anion transportation. Excessive water uptake, however, results in serious swelling, making the membranes mechanically too weak for AEM applications. The water uptake in the crosslinked BI-cPES membranes was measured at 20 °C and 80 °C (Table 3). As expected, crosslinking effectively suppressed swelling, and the water uptake in all crosslinked BI-cPES membranes was very low (<12%), even at 80 °C, indicating that the membranes retained their flexibility in water even at high temperatures. The lowest water uptake was observed for BI-cPES-10, which formed a self-aggregated structure that inhibited water uptake.

Water uptake and conductivity (σ) are particularly important for fuel cell applications, and the comb-shaped bisimidazolium-mediated crosslinked BI-cPES-10 membrane, which displayed an extremely high conductivity with a very low water uptake, offers an ideal material for AEM fuel cell applications.

Table 3. Water uptake and dimensional stability for the crosslinked BI-cPES membranes.

Membrane	Water uptake (%)		Swelling ratio (Δt)	
	20 °C	80 °C	20 °C	80 °C
BI-CPES-4	9.40	11.3	5.20	7.10
BI-CPES-6	9.10	10.6	5.50	6.98
BI-CPES-10	8.70	9.90	4.90	6.75

The dimensional stabilities of the crosslinked BI-cPES membranes were further evaluated, and all crosslinked BI-cPES membranes revealed very low swelling, as expected (Table 3). Increasing the alkyl chain length of the bisimidazolium cation reduced the swelling, and the lowest swelling was obtained for BI-cPES-10 due to the combined effects of the crosslinked 3-D network and the self-aggregated structure formed by the comb-shaped polymer (BI-cPES-10).

Thermal and mechanical properties

The thermal stabilities of the crosslinked BI-cPES membranes in their hydroxide form were evaluated by thermogravimetric (TGA) analysis (Figure 5). The initial slight weight loss of less than 3% was attributed to the evaporation of hydrated water or residual solvent. A two-step weight loss was then followed for all three crosslinked membranes. The first weight loss observed at 340–450°C corresponded to the loss of imidazolium groups. The second stage of weight loss from 470 °C corresponded to the decomposition of the polymer side chains and main chains. The bisimidazolium-mediated crosslinked BI-cPES membranes displayed a high thermal stability compared to typical crosslinked quaternary ammonium or quaternary guanidinium cations. A high thermal stability is preferred for AEM fuel cells to reduce thermodynamic voltage losses caused by pH value differences across the membrane. These results suggested that the introduction of alkyl bisimidazole as a crosslinker enhanced the

thermal stability and preserved the high rigidity of the polymer backbone.

Figure 5 here

In addition to a high thermal stability, AEMs must also have sufficient mechanical strength for use in the fabrication of MEAs. The mechanical properties of crosslinked BI-cPES membranes were evaluated and compared with that of the Br-PES at 50% RH (Figure 6 and Table S2 in ESI[†]). The bisimidazolium-mediated crosslinked membranes showed decrease in elongation but high Young's modulus in the range 2.1–3.9 GPa. The Young's modulus increased with the alkyl chain length between the two imidazolium groups, with the highest value obtained for BI-cPES-10 (2.1 GPa for BI-cPES-4, 2.4 GPa for BI-cPES-6, and 3.9 GPa for BI-cPES-10) due to the formation of a self-aggregated structure in this crosslinked comb-shaped polymer membrane (BI-cPES-10).

Figure 6 here

Chemical and oxidative stability

The long-term alkaline stabilities of the crosslinked BI-cPES membranes were evaluated by comparing the conductivities and IEC values before and after immersing the membranes in a 2 M NaOH solution at 60 °C for 350 h (Figure 7). The changes in conductivity were measured at 20 °C every 48 h, and the conductivities of all three crosslinked BI-cPES membranes decreased slightly from their original conductivity after thermal treatment under basic conditions. No significant changes in the conductivity were observed up to 200 h, after which a slight decrease in the IEC and conductivity was observed (Table 4 and Figure 7). The alkaline stabilities of these crosslinked BI-cPES membranes were very high, in contrast with typical AEMs, which are generally unstable under these conditions (concentrated basic solutions at high temperatures) [50].

Figure 7 here

Table 4. Conductivities and IEC values of the crosslinked BI-cPES membranes before and after soaking in 2 M NaOH at 60 °C for 350 h.

Membrane	Conductivity at 20°C (S/cm)		IEC (meq/g)	
	Before	After	Before	After
BI-cPES-4	0.012	0.008	1.20	1.13±0.02
BI-cPES-6	0.016	0.012	1.18	1.11±0.02
BI-cPES-10	0.027	0.022	1.13	1.05±0.02

The bisimidazolium-mediated crosslinked membranes (BI-cPES-4, BI-cPEs-6 and BI-cPES-10) were further analyzed structurally by comparing the IR spectra before and after exposure to thermal treatment under basic conditions to monitor any degradation of the bisimidazolium groups and the polymer backbone (Figure S5 in ESI[†]). No significant changes in these membranes were observed, as the characteristic peaks at 1590 cm^{−1} and 758 cm^{−1}, corresponding to the imidazolium groups, remained intact. Therefore, the structural integrity of the BI-cPES membranes was maintained even in the presence of harsh alkaline conditions.

The mechanical properties of the crosslinked membranes after alkaline stability test were also compared with those before the alkaline stability test. As shown in both Figure S6 and Table S3 in ESI[†], all the crosslinked membranes experienced decrease in their original mechanical properties, but still maintained their flexibility.

The oxidative stability of all the crosslinked membranes was further evaluated by monitoring the weight loss of the corresponding membranes in Fenton's reagents at 60 °C for 250 h, and the results were compared with that of the non-crosslinked membrane (Br-PES) (Figure S7 in ESI[†]).[51,52] While the Br-PES membrane was broken into pieces only after 50 h under these conditions, the crosslinked BI-cPES membranes experienced gradual weight loss but retained their flexibility up to 250 h. After this time they were also broken into pieces. These results indicate that the crosslinked membranes (BI-cPES) significantly improved the oxidative stability of AEMs. In addition, the weight loss of the BI-cPES-10, having the longest alkyl chain, was lower than the BI-cPES-4 and BI-cPES-6, due to the formation of the self-aggregated structure.

Conclusions

We synthesized alkyl bisimidazolium-mediated crosslinked poly(arylene ether sulfone) block copolymers with alkyl chains that varied in length from C_4 to C_{10} as novel anion exchange membranes. The alkyl bisimidazolium groups were used both as crosslinkers and ion conductors for the first time. The bisimidazolium-mediated crosslinked BI-cPES membranes outperformed typical AEMs and belong among the limited number of crosslinked membranes having both a high conductivity and good dimensional stability. The BI-cPES membrane with long alkyl chains (C10, BI-cPES-10) formed a self-aggregated structure due to the presence of the long pendant hydrophobic side chains, which conveyed a comb shape to the polymer. The crosslinked comb-shaped system displayed very high conductivity, even at low IEC values, and a low water uptake. The combination of comb-shaped long chains, together with the crosslinked network, indicated that BI-cPES-10 is an excellent candidate electrolyte for use in AEM fuel cells.

Notes and references

[a]Organic Material Synthesis Laboratory, Department of Chemistry, Incheon National University, Incheon,406-772, Korea. E-mail: tkim@inu.ac.kr; Fax: +82-32-835-0762; Tel: +82-32-835-8232
[b]Department of Materials Engineering and Convergence Technology, Engineering Research Institute, Gyeongsang National University, Jinju 660-701, Korea.
†Electronic Supplementary Information (ESI) available: [details of ^{1}H NMR, IR spectra, gel fraction, solubility and stress-strain curve data]. See DOI: 10.1039/b000000x/

1   J. R. Varcoe, P. Atanassov, D. R. Dekel, A. M. Herring, M. A. Hickner, P. A. Kohl, A. R. Kucernak, W. E. Mustain, K. Nijmeijer, K. Scott, T. Xu and L. Zhuang, *Energy Environ. Sci.*, 2014, **7**, 3135-3191.

2   G. Merle, M. Wessling and K. Nijmeijer, *J. Membr. Sci.*, 2011, **377**, 1-35.

3   J. S. Spendelow and A. Wieckowski, *Phys. Chem. Chem. Phys.*, 2007, **9**, 2654-2675.

4   J. R. Varcoe and R. C. T. Slade, *Fuel cells*, 2005, **5**, 187-199.

5   Z. Zhao, J. Wang, S. Li and S. Zhang, *J. Power. Sources*, 2011, **196**, 4445-4450.

6   X. Li, Q. Liu, Y. Yu and Y. Meng, *J. Membr.Sci.*, 2014, **467**, 1-12.

7   Z. Liu, X. Li, K. Shen, P. Feng, Y, Zhang, X. Xu, W. Hu, Z. Jiang, B. Liu and M. D. Guiver, *J. Mater. Chem. A*, 2013, **1**, 6481-6488.

8   H. Zarrin, J. Wu, M. Fowler and Z. Chen, *J. Membr. Sci.*, 2012, **394-395**, 193-201.

9   G. Wang, Y. Weng, J. Zhao, R. Chen and D. Xie,. *J. Appl. Polym. Sci.*, 2009, **112**, 721-727.

10   L. Wu, T. Xu, D. Wu and X. Zheng, *J. Membr. Sci.*, 2008, **310**, 577-585.

11   X. Lin, L. Wu, Y. Liu, A. L. Ong, S. D. Poynton and J. R. Varcoe, *J. Power. Sources*, 2012, **217**, 373-380.

12   Q. Li, L. Liu, Q. Miao, B. Jin and R. Bai, *Chem. Commun.,* 2014, **50**, 2791-2793.

13   R. Vinodh, M. Purushothaman and D. Sangeetha, *Int. J. Hydrogen Energy*, 2011, **36**, 7291-7302.

14   X. Yan, G. He, S. Gu, X. Wu, L. Du and H. Zhang, *J. Membr. Sci.,* 2011, **375**, 204-211.

15   J. Wang, J. Wang, S. Li and S. Zhang, *J. Membr. Sci.*, 2011, **368**, 246-253.

16   Z. Qiang, Z. Qifeng, W, Junhua, Z. Suobo and S. Li, *Polymer*, 2010, **51**, 5407-5416.

17   J. Wang, S. Li and S. Zhang, *Macromolecules*, 2010, **43**, 3890-3896.

18   M. Jung, C. G. Arges and V. Ramani, *J. Mater. Chem.*, 2011, **21**, 6158-6160.

19   S.-J. Hahn, M. Won and T.-H. Kim, *Polym. Bull.*, 2013, **70**, 3373-3385.

20   F. Zhang, H. Zhang and C. Qu, *J. Mater. Chem.*, 2011, **21**, 12744-12752.

21   X. Yan, G. He, S. Gu, X. Wu, L. Du and Y. Wang, *Int. J. Hydrogen Energy*, 2012, **37**, 5216-5224.

22   A. H. N. Rao, R. L. Thankamony H.–J. Kim, S. Nam and T.-H. Kim, *Polymer*, 2013, **54**, 111-119.

23   A. H. N. Rao, H.-J. Kim, S. Nam and T.-H. Kim, *Polymer*, 2013, **54**, 6918-6928.

24   A. H. N. Rao, S. Nam and T.–H. Kim, *J. Mater. Chem. A*, 2015, **3**, 8571-8580.

25   J. Kerres, *J. Membr. Sci.*, 2001, **185**, 3-27.

26   Y. Zhu, S. Zieren and A. Manthiram, *Chem. Commun.,* 2011, **47**, 7410-7412.

27   J. Kerres, W. Zhang, L. Jorissen and V. Gogel,. *J. New Mat. Electrochem. Systems*, 2002, **5**, 97-107.

28   J. Pan, Y. Li, L. Zhuang and J. Lu, *Chem. Commun.*, 2010, **45**, 8597-8599.

29   Y. Z. Zhuo, A. N. Lai, Q. G. Zhang, A. M. Zhu, M. L. Ye and Q. L. Liu, *J. Membr. Sci.*, 2015, **491**, 138-148.

30   S. H. Tian, Y. Z. Meng and A. S. Hay, *Macromolecules,* 2009, **42**, 1153-1160.

31   K. Matsumoto, T. Higashihara and M. Ueda, *Macromolecules*, 2009, **42**, 1161-1166.

32   Y.–S. Oh, H.–J. Lee, M. Yoo, H.–J. Kim, J. Han and T.–H. Kim, *Chem. Commun.*, 2008, **17**, 2028-2030.

33   T. Yamaguchi, H. Zhou, S. Nakazawa and N. Hara, *Adv. Mater.*, 2007, **19**, 592-596.

34   A. A. Argun, J. Ashcraft and P. T. Hammond, *Adv. Mater.*, 2008, **20**, 1539-1543.

35   S. Gu, R. Cai, T. Luo, Z. W. Chen, M. W. Sun, Y. Liu, G. H. He and Y. S. Yan, *Angew. Chem., Int. Ed.*, 2009, **121**, 6621-6624.

36   N. Li, T. Yan, Z. Li, T. T. Albrecht and W. H. Binder, *Energy Environ. Sci.*, 2012, **5**, 7888-7892.

37   N. Li, Y. Leng, M. A. Hickner and C.-Y. Wang, *J. Am. Chem. Soc.*, 2013, **135**, 10124-10133.

38   J. Ran, L. Wu and T. Xu, *Polym. Chem.*, 2013, **4**, 4612-4620.

39   J. Pan, C. Chen, L. Zhuang and J. Lu, *Acc. Chem. Res.*, 2012, 45, 473-481.

40   M. Yang, K. Stappert and A.–V. Mudring, *J. Mater. Chem. C*, 2014, **2**, 458-473.

41   G. Chen, X. Zhang, S. Zhang, T. Chen and Y. Wu, *J. Appl. Polym. Sci.*, 2007, **106**, 2808-2816.

42   B. Lin, L. Qiu, B. Qiu, Y. Peng and F. Yan, *Macromolecules*, 2011, **44**, 9642-9649.

43   J. Ran, L. Wu, J. R. Varcoe, A. L. Ong, S. D. Poynton and T. Xu, *J. Membr. Sci.*, 2012, **415-416**, 242-249.

44   G. L. Han, P. Y. Xu, K. Zhou, Q. G. Zhang, A. M. Zhu and Q. L. Liu, *J. Membr. Sci.*, 2014, **464**, 72-79.

45   S. Min and D. Kim, *Solid State Ionics*, 2010, **180**, 1690-1693.

46   S. Xu, G. Zhang, Y. Zhang, C. Zhao, L. Zhang, M. Li, J. Wang, N. Zhang and H. Na, *J. Mater. Chem.*, 2012, **22**, 13295-13302.

47   J. Zhou, M. Unlu, I. A-Richard and P. A. Kohl, *J. Membr. Sci.*, 2010, **350**, 286-292.

48   G. Nie, X. Li, J. Tao, W. Wu and S. Liao, *J. Membr. Sci.*, 2015, **474**, 187-195.

49   T.–H. Tsai, S. P. ertem, A. M. Maes, S. Seifert, A. M. Herring and E. B. Coughlin, *Macromolecules*, 2015, **48**, 655-662.

50   D. Chen and M. A. Hickner, *ACS Appl. Mater. Interfaces*, 2012, **4**, 5775-5781.

51   T. Chakrabarty, S. Prakash and V. K. Shahi, *J. Membr. Sci.*, 2013, **428**, 86-94.

52   K. Shen, Z. Zhang, H. Zhang, J. Pang and Z. Jiang, *J. Power Sources*, 2015, **287**, 439-447.
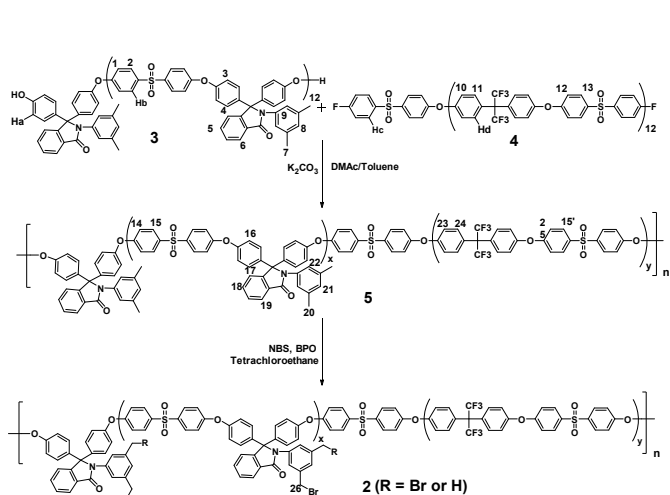
Scheme 1. Synthesis of the bromobenzylated poly(arylene ether sulfone) block copolymer (Br-PES) **2**
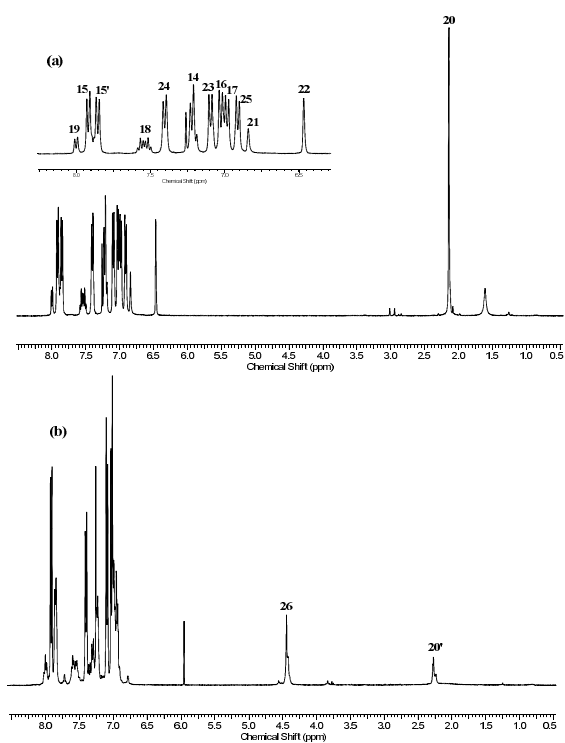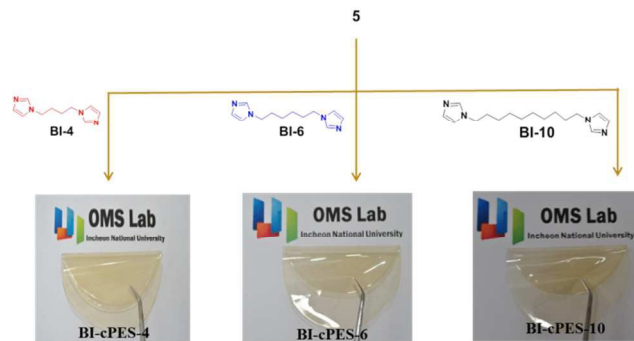

Scheme 2. Preparation of the bisimidazolium-mediated crosslinked membranes with alkyl chain lengths of C_4 (BI-cPES-4), C_6 (BI-cPES-6), and C_{10} (BI-cPES-10)
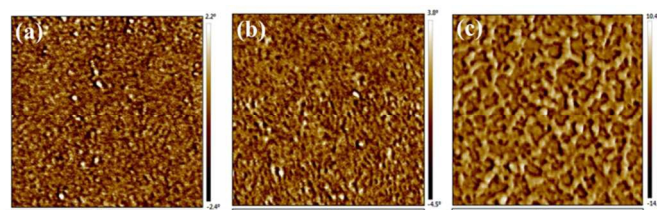

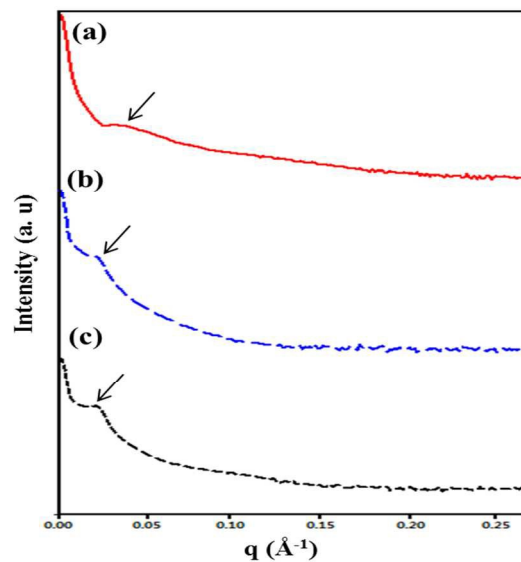**Figure 2.** AFM images of BI-cPES-4 (a), BI-cPES-6 (b), and BI-cPES-10 (c)

Figure 1. ^{1}H NMR spectra of the PES block copolymer (**5**) (a) and brominated PES (Br-PES, **2**) (b) in CDCl$_3$

Figure 3. SAXS profiles of BI-cPES-4 (a), BI-cPES-6 (b), and BI-cPES-10 (c)
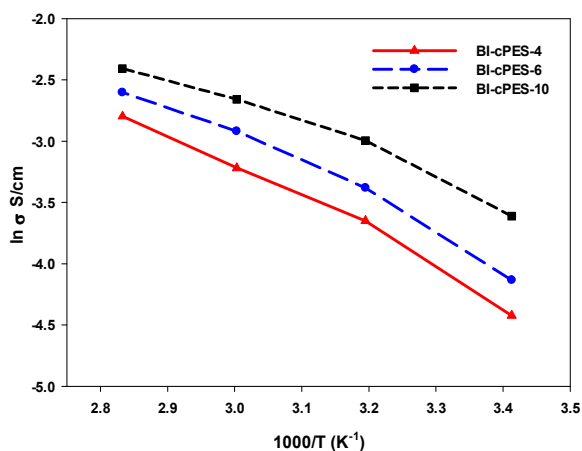
Figure 4. Arrhenius plots of the conductivity *versus* temperature in the crosslinked BI-cPES membranes at 100% RH
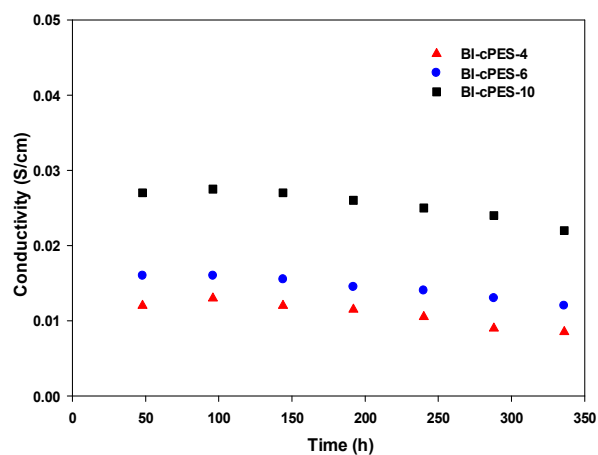

Figure 7. Conductivity of the BI-cPES membranes after soaking in 2 M NaOH at 60°C for 350 h
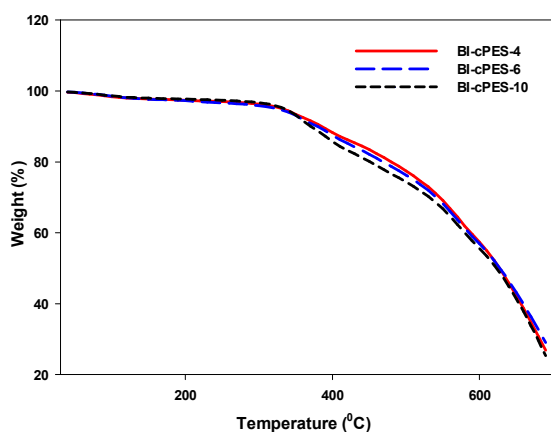

Figure 5. TGA thermograms of the crosslinked BI-cPES membranes
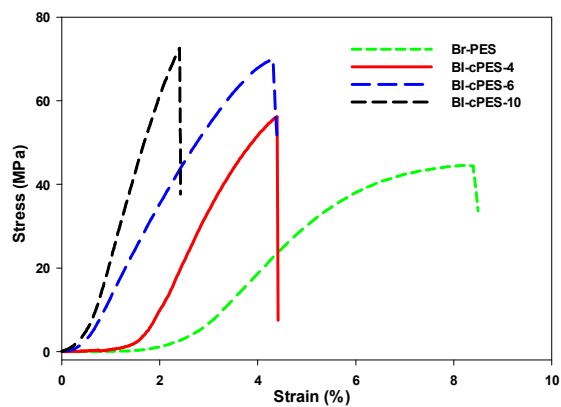

Figure 6. Stress–strain curves of the crosslinked BI-cPES membranes and their precursor (Br-PES) in the dry state

RSC Advances Accepted Manuscript

1